

Cross-Linked Surface Engineering to Improve Iron Porphyrin Catalytic Activity

Dongxu Zhang, Jia Liu, Peiyao Du, Zhen Zhang, Xingming Ning, Yang Deng, Dan Yin, Jing Chen, Zhengang Han, and Xiaoquan Lu*

Quasi-two-dimensional (QTD) structural heterogeneous catalysts have attracted a broad interest in multidisciplinary research due to their unique structure, preeminent surface properties and outstanding catalytic performance. Herein, a HZIF@TCPP-Fe/Fe heterogeneous catalyst based on cross-linked surface engineering is constructed by supporting QTD TCPP-Fe/Fe ultra-thin metallized film (≈ 2 nm) on hollow skeleton of zeolite imidazolate frameworks. The designed QTD structure exhibits high efficiency for the catalytic oxidative dehydrogenation of aromatic hydrazides reactions which is the key technology in various industrial processes. Taking advantage of QTD structure with excellent accessibility, the metallized film with irregular defects not only enhances electron transfer during the reaction but also exposes more surface-active sites. Furthermore, the prepared HZIF@TCPP-Fe/Fe heterogeneous catalyst can be recycled and reused, which is of great significance in the field of green chemistry.

Nanoreactors, with controllable elaborate microstructure, ideal local voids, and hollow nanostructures, show excellent performance on catalysis, supercapacitors, chemical sensors, and biomedicine.^[1–5] Particularly, for catalysis, the well-designed hollow nanomaterials do not only provide platform for the specific catalytic reaction but also can be used as model to reveal the mechanism of nano-catalytic reaction. Generally, metal organic frameworks (MOFs) have shown a lot of advantages as an important type of catalyst and have emerged as promising platforms for diverse applications.^[6–10] However, the microporous structure property of MOFs hinders the large-scale molecules entering their internal pores, and in some cases significantly limits their application in the catalytic field. As such, using of MOFs as a hard-template is a

straightforward and universal method for obtaining hollow nanostructures and, the hollow nanostructures can be acted as a skeleton for heterogeneous catalysts to catalyze specific reactions.^[11] Distinctively, construction of quasi-two-dimensional (QTD) porous solid based MOFs film is one of most efficiency strategy to endow materials with desired surface properties (e.g., permeability, adhesion, erosion, elasticity, and photoelectric properties) and large-scale contactable active sites, but still a challenge until now. Suboptimal controllability and complexity of synthesis, finiteness of available MOFs resources as well as poor stability are the main obstacles hinder QTD film based material's application. We proposed an alternate of QTD

ultra-thin metallized film by depositing organic ligands and metal nodes on a hollow skeleton combined with the external cross-linked surface engineering, typically by post-synthetic modification (PSM) methodologies, for tuning the chemical and physical properties which determines their performance in catalysis.^[12–14] As a consequence, the heterogeneous catalyst having a QTD film structure combines the merits of homogeneous and heterogeneous catalyst, which can be sufficiently contacted with a reactant and easily separated and recovered. Heterogenization of homogeneous metal complex catalysts occurs in some simple steps due to the coordination mechanism involved, and it provides a method for anchoring specific functional molecules into the catalyst structure without compromising the integrity of the framework structure.^[15] With the development of controllable synthesis methods, a large number of functionalization methods have been used to implement the catalysts design, such as: “single site” immobilized,^[16,17] variants and sequences introduced,^[18–20] and catalytic environment coordinated.^[21,22] Herein, the QTD film is deposited on the surface of the hollow skeleton, so that the ultra-thin metallized film has inherent stability compared with the traditional 2D analog, and its catalytic activity can be fully demonstrated. Therefore, this method has broad prospects in the preparation of heterogeneous catalysts.

Recently, metal-complex with specific catalytic activity have been immobilized on various carrier surfaces to construct organic/inorganic interfaces by surface molecular engineering to form a solid catalytic center with a clear chemical structure and function, thereby converting a homogeneous catalytic reaction into a heterogeneous catalytic reaction,

D. Zhang, Dr. J. Liu, Dr. P. Du, Dr. Z. Zhang, X. Ning, Y. Deng, D. Yin, Prof. X. Lu

Tianjin Key Laboratory of Molecular Optoelectronic Science
Department of Chemistry School of Science

Tianjin University

Tianjin 300072, P. R. China

E-mail: luxq@tju.edu.cn, luxq@nwnu.edu.cn

Dr. J. Chen, Dr. Z. Han, Prof. X. Lu

Key Laboratory of Bioelectrochemistry & Environmental Analysis
of Gansu Province

College of Chemistry and Chemical Engineering

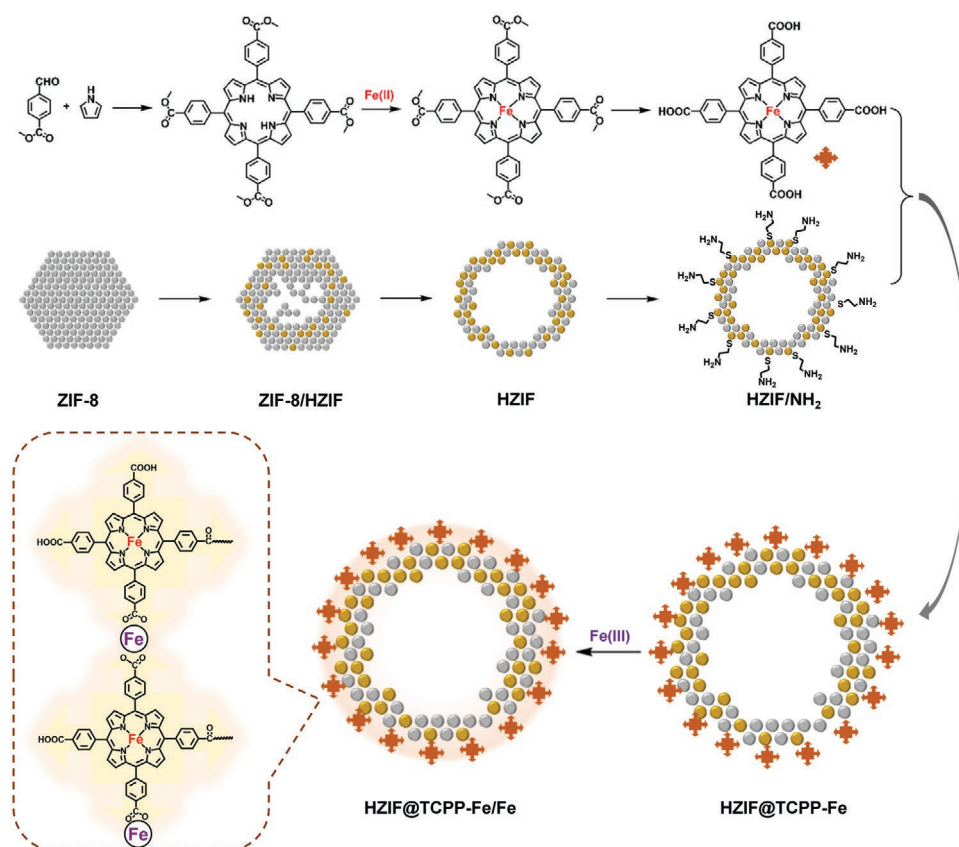
Northwest Normal University

Lanzhou 730070, P. R. China



The ORCID identification number(s) for the author(s) of this article can be found under <https://doi.org/10.1002/smll.201905889>.

DOI: 10.1002/smll.201905889



Scheme 1. Design strategy to synthesize HZIF@TCPP-Fe/Fe heterogeneous catalyst.

improving catalytic efficiency, and solving the problem of catalysts recovery.^[23–27] Taking account of advantages and unique properties of metal-porphyrins such as excellent electron donors with delocalized π systems, rigid and planar geometry, high thermal stability, high electron stability, small band, adjustable band gap, excellent optical, and ideal redox behavior,^[28–31] a type of tetrakis(4-carboxyphenyl)-porphyrin-Fe (TCPP-Fe) based QTD ultra-thin metallized film materials was constructed by in-situ deposition of TCPP-Fe molecule chelated with iron ions (Fe(III)) on the surface of hollow nanocages by cross-linked surface engineering. Our aim is to improve the catalytic performance of HZIF@TCPP-Fe/Fe catalyst on oxidative dehydrogenation of aromatic hydrazides and investigate the basic mechanism. The larger voids provided by irregular defects in metallized films as the “holes” can effectively enhance the accessibility of active sites, which is conducive to improving their catalytic activity.^[32–34] Hence, the unique QTD ultra-thin metallized film structural cross-linked on the surface of hollow skeleton generally exhibits higher catalytic performance than their monomer presence counterparts, mainly due to stabilization of the films through immobilization, the electron deficient iron-oxo complexes are much better electron acceptors, they will be more powerful oxidants than the corresponding species derived from non-metal porphyrin molecule, and it can effectively enhance the catalytic activity of porphyrin-Fe by cross-linked surface engineering.

The main synthesis steps are briefly described as shown in **Scheme 1**. By cation exchange with Au^{3+} ions, the homometallic zeolite imidazolate frameworks-8 (ZIF-8) nanoparticles transform into hollow ZIF (HZIF) nanocages skeleton due to Kirkendall effect.^[35] The Au and Zn focus mostly on the shell of the as-prepared HZIF nanocage, and the β -mercaptoethylamine were anchored on the Au atom to form an amino-functional ($-\text{NH}_2$) hollow ZIF-8 (HZIF/ NH_2) skeleton. The exposed $-\text{NH}_2$ group on the surface bind with TCPP-Fe to construct an organic/inorganic interface to form a HZIF@TCPP-Fe catalyst precursor. After adding Fe(III) ions, the TCPP-Fe cross-linked via the coordination interaction between Fe(III) and carboxyl group ($-\text{COOH}$) of TCPP to form QTD ultra-thin metallized film on the surface of HZIF/ NH_2 skeleton. As an ideal heterogeneous carrier, HZIF/ NH_2 skeleton effectively supports the TCPP-Fe/Fe ultra-thin metallized film, which exposed large amount of isolated catalytic active sites for reactants easily approaching. The synthesis routes and structure details of TCPP-Fe are described in the Supporting Information (Figures S1–S5, Supporting Information).

Transmission electron microscopy (TEM) image (**Figure 1a**) shows obviously hollow structure of HZIF@TCPP-Fe/Fe. The shell thickness is about 20 nm determined by the high-resolution transmission electron microscope (HR-TEM), as shown in **Figure 1b**. It also can be observed that the QTD TCPP-Fe/Fe ultra-thin metallized film is about 2 nm with clearly edge as shown in **Figure 1c**. Some defects can also be identified in

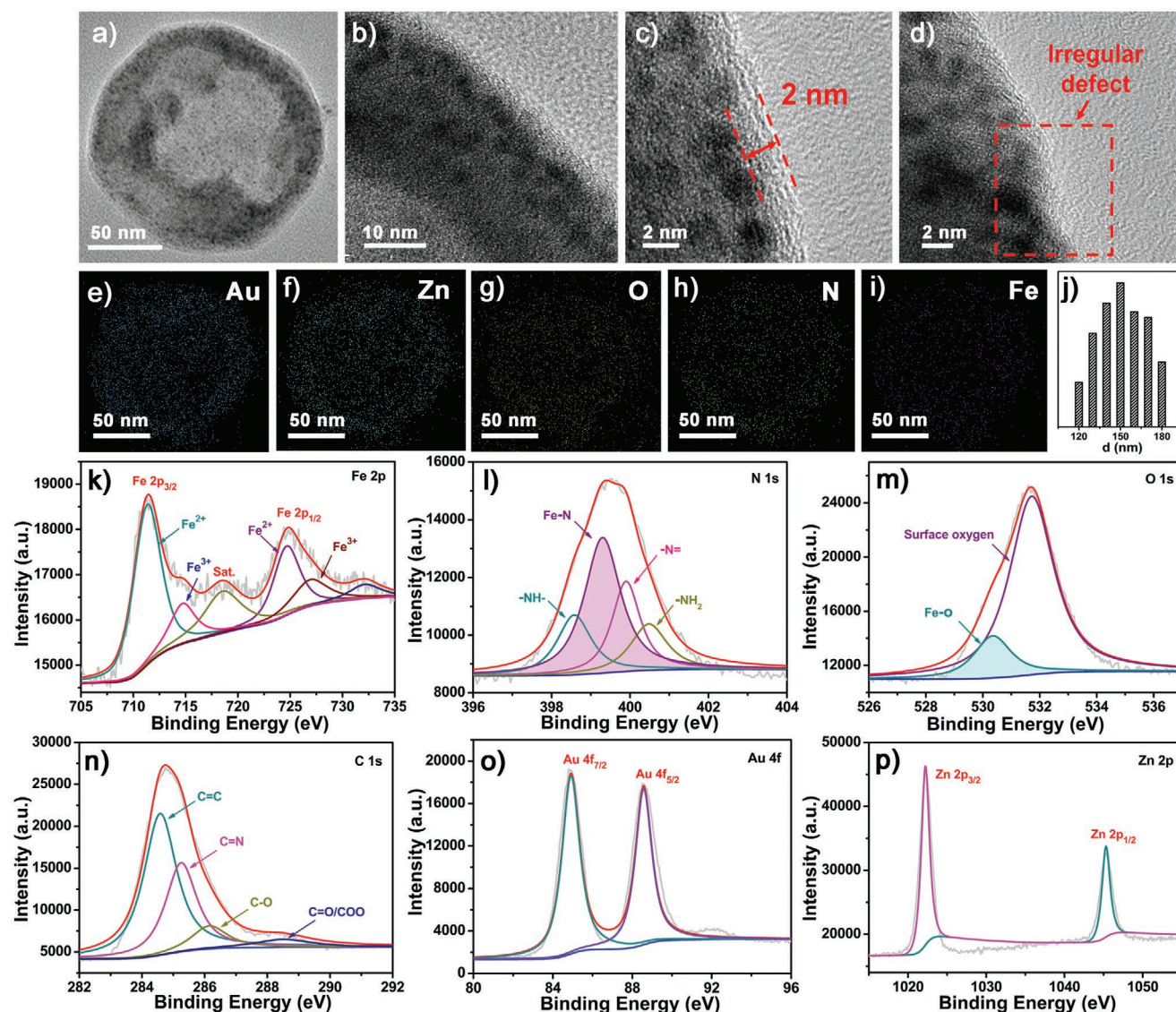


Figure 1. a) TEM images of HZIF@TCPP-Fe/Fe. b–d) HR-TEM images of HZIF@TCPP-Fe/Fe. e–i) EDS elemental (Au, Zn, O, N, and Fe) mapping of HZIF@TCPP-Fe/Fe. j) Diameter distribution histogram of HZIF@TCPP-Fe/Fe. High-resolution XPS spectra of k) Fe 2p, l) N 1s, m) O 1s, n) C 1s, o) Au 4f, and p) Zn 2p of HZIF@TCPP-Fe/Fe.

Figure 1d indicate that the cross-linked TCPP-Fe/Fe film does not full cover the surface of hollow ZIF-8 skeleton. Energy dispersive spectrometer (EDS) mappings (Figure 1e–i) indicate the elements distributing uniformly. The as-synthesized HZIF@TCPP-Fe/Fe presents a relatively uniform diameter of 150 ± 30 nm (Figure 1j). During the preparation process, collapse or large-scale aggregations did not occur, at the same time, no metallized film existed on the surface of the HZIF@TCPP-Fe catalyst precursor, which can be confirmed by scanning electron microscope (SEM) and TEM images (Figure S6a–j, Supporting Information). The large-field SEM images, EDS mappings (Figure S7, Supporting Information) and Fourier transform infrared spectroscopy (FT-IR) spectra (Figure S8, Supporting Information) show no obvious change indicating the structural integrity of the material, which ensure their original excellent properties were retained.^[36] In addition, regarding

the relationship between TCPP-Fe and Fe(III), the above two were directly mixed, unexpectedly, a large number of precipitates (TCPP-Fe/Fe bulk complex) with irregular shapes were generated, and uniform QTD TCPP-Fe/Fe ultra-thin metallized film cannot be achieved (Figure S9, Supporting Information).

To investigate the chemical composition and oxidation states of the as-synthesized nanocomposites, X-ray photoelectron spectroscopy (XPS) analysis were performed. The survey spectra of the HZIF@TCPP-Fe/Fe was shown in Figure S10, Supporting Information. High-resolution Fe 2p spectrum of HZIF@TCPP-Fe/Fe could be deconvoluted into five peaks at 710.4, 714.8, 718.6, 724.7, and 727.9 eV, which were attributed to the Fe(II) 2p_{3/2}, Fe(III) 2p_{3/2}, satellite, Fe(II) 2p_{1/2}, and Fe(III) 2p_{1/2} peak, respectively, suggesting that Fe existed as Fe(II) and Fe(III) in the possible form of HZIF@TCPP-Fe/Fe (Figure 1k).^[37–39] High-resolution XPS spectra of N 1s, C 1s, and O 1s deconvoluted into

the peaks at 399.3 and 530.2 eV, corresponding to Fe–N and Fe–O (Figure 1i–n).^[40,41] The XPS spectra of Au 4f and Zn 2p as shown in Figure 1o,p.^[42,43] Comparing with the XPS spectra of HZIF@TCPP-Fe (Figure S11, Supporting Information), the appearance of peak at 714.8 eV indicates the successful embedding of Fe(III). The mole ratio of Fe in HZIF@TCPP-Fe and HZIF@TCPP-Fe/Fe is about 1/1.5 calculated by the result of inductively coupled plasma mass spectrometry (ICP-MS) (Table S1, Supporting Information). The type of porphyrin-Fe based QTD materials by in-situ deposition of TCPP-Fe molecule chelated with Fe(III) on the surface of hollow nanocages by cross-linked surface engineering was successfully constructed.

X-ray powder diffraction (XRD) was measured to verify the composition and structural information. It can be derived that the as-prepared HZIF@TCPP-Fe/Fe maintains well-resolved diffraction peaks corresponding to ZIF-8 (Figure 2a). In addition, we optimized the amount of Fe(III) added. After a cross-linked surface engineering treatment, the XRD peaks are identical to pure ZIF-8 (Figure S12, Supporting Information). The thermal stabilities of as-prepared materials were studied by using thermogravimetric analysis (TGA). As shown in Figure 2b, the TGA profile taken in the nitrogen of HZIF@TCPP-Fe/Fe suggests the nanocages structures are stable up to 230 °C. The obviously weight loss occurred in the temperature range of 230 and 450 °C is ascribed to the decomposition of TCPP-Fe and 2-methylimidazole from the HZIF@TCPP-Fe/Fe. The UV-vis absorption spectra of HZIF@TCPP-Fe and HZIF@TCPP-Fe/Fe displayed new bands attributed to the Soret band (424 nm) and the Q bands (577, 630, and 691 nm) of the TCPP-Fe units respectively, which proved that the TCPP-Fe was successfully supported on the surface of the hollow skeleton and the relative intensity increased with the formation of QTD TCPP-Fe/Fe ultra-thin

metallized film (Figure 2c). To obtain the porous structure information of the desolated ZIF-8, HZIF@TCPP-Fe, and HZIF@TCPP-Fe/Fe, the N₂ adsorption-desorption isotherms were measured at 77 K, as displayed in Figure 2d. These materials exhibit Brunauer–Emmett–Teller (BET) surface of 1739, 788, and 140 m²g^{−1}, respectively. The large hysteresis loop appeared on the latter two materials at high pressure can be attributed to the hollow structure. Moreover, significant decrease in surface area was observed for the HZIF@TCPP-Fe/Fe, which prove that the formation of the metallized film blocks micropores of the hollow skeleton and indicate that QTD TCPP-Fe/Fe ultra-thin metallized film was successfully constructed and possessed high density and rich catalytically active sites. Furthermore, the time-resolved photoluminescence (TRPL) spectroscopy is a very important means to understand the quenching mechanism of TCPP-Fe in cooperation with Fe(III). The results illustrated that excited-state molecules of TCPP-Fe interacted with Fe(III) in the outer surface of HZIF/NH₂, because the average emission lifetime was reduced from 28.439 to 16.792 ns (Figure 2e see also Table S2, Supporting Information).

Aromatic azo compounds are widely used in the chemical industry, it is of great significance for people to explore highly-efficient catalysts and apply it widely in the field of azo compounds production.^[44] As a number of prior reports have already described the preparation of aromatic azo compounds using iron (II) phthalocyanine (Fe(Pc)) as the catalyst.^[45–49] To our knowledge, Fe(Pc) as catalyst has great potential as oxidation catalysts, however, the Fe(Pc) molecule cannot be recycled, resulting in a significant waste and environmental pollution. Against this backdrop, we particularly focus on the cross-linked surface engineering with respect to the hollow skeleton for the rational design of heterogeneous catalysts in terms of

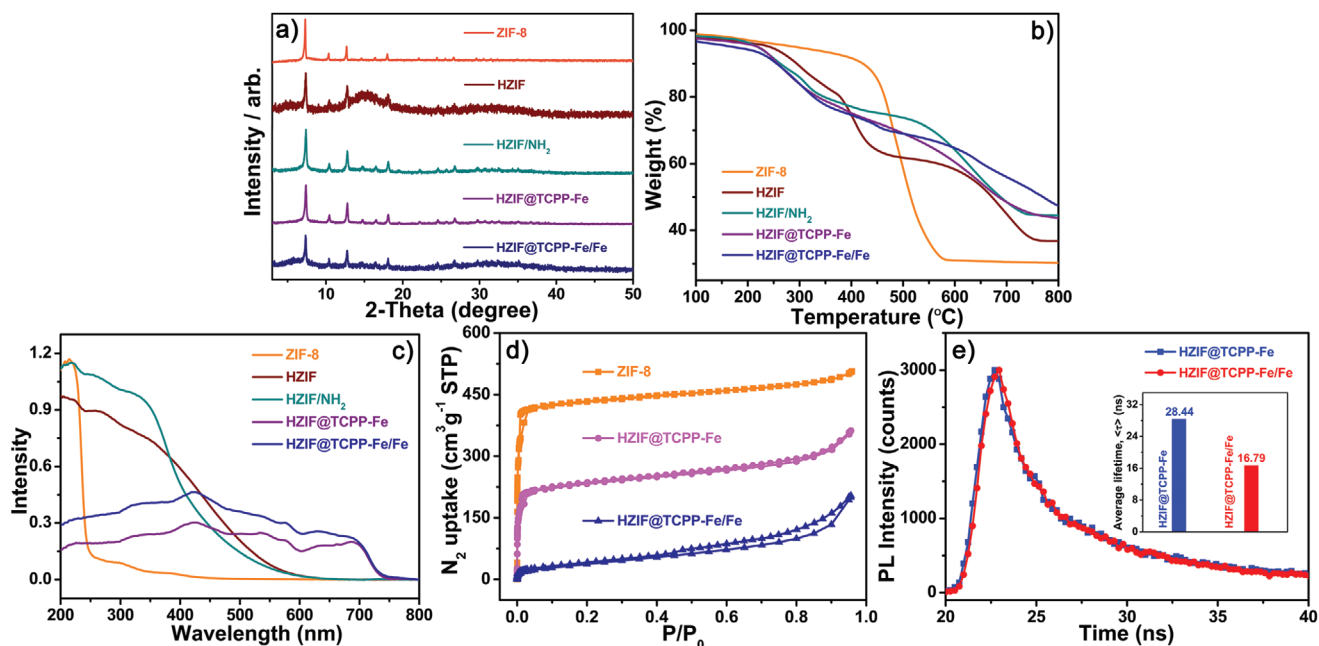


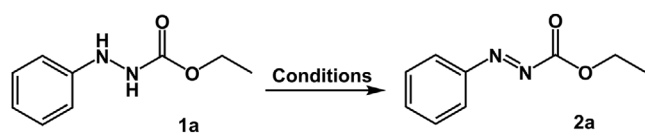
Figure 2. a) Powder XRD patterns for ZIF-8, HZIF, HZIF/NH₂, HZIF@TCPP-Fe, and HZIF@TCPP-Fe/Fe. b) TGA profiles of ZIF-8, HZIF, HZIF/NH₂, HZIF@TCPP-Fe, and HZIF@TCPP-Fe/Fe in N₂ atmosphere. c) UV-vis spectra of ZIF-8, HZIF, HZIF/NH₂, HZIF@TCPP-Fe, and HZIF@TCPP-Fe/Fe (powder sample). d) N₂ sorption isotherms at 77 K of ZIF-8, HZIF@TCPP-Fe and HZIF@TCPP-Fe/Fe. e) Time-resolved photoluminescence emission decay spectra of HZIF@TCPP-Fe and HZIF@TCPP-Fe/Fe.

functionalization methods and structure correlated catalysis. Compared with structure-related Fe(Pc), the catalytic performance of porphyrin-Fe complexes for catalyzing the oxidative dehydrogenation of aromatic hydrazides to azo products has not been fully studied. It is noticeable that TCPP-Fe molecules can be used as oxidation catalysts, and the combination of TCPP-Fe and atmospheric oxygen would be conceptually ideal to realize practical oxidation methods.^[50,51] Since TCPP-Fe was capable to catalyze the oxidative dehydrogenation of aromatic hydrazide, therefore, a novel method for the preparation of QTD TCPP-Fe/Fe ultra-thin metallized film was further developed. In this work, we deeply explored the oxidative dehydrogenation of aromatic hydrazide in detail, including optimization of catalytic conditions and investigation of reaction mechanism. When a mixture of ethyl 2-phenylhydrazine-1-carboxylate (1a) and a catalytic amount of as prepared HZIF@TCPP-Fe/Fe heterogeneous catalyst (5 mol %) was exposed to atmospheric oxygen, ethyl 2-phenyldiazene-1-carboxylate (2a) was obtained in good yield (92%) in a shorter reaction time (4 h) after purification by chromatography compared to the porphyrin catalysts (Fe(Tpp)Cl) reported in the literature.^[52] The reaction was neither induced in absence of the catalyst nor presence of only hollow skeleton without TCPP-Fe units (Table 1, Entries 1–4). Next, replacement of TCPP-Fe with other different coordination modes of iron (HZIF@Fe(II), HZIF@Fe(III), FeCl₂·4H₂O, and

FeCl₃·6H₂O) were tested (Table 1, Entries 5–8). All above catalysts have no significant catalytic effect, which prove that the iron salt supported on the surface or pore of the hollow skeleton does not play a major role in the HZIF@TCPP-Fe/Fe catalyst. HZIF@TCPP-Fe catalyst precursor with TCPP-Fe units have the potential ability to act as catalysts for activation of molecular oxygen (Table 1, Entry 9). The THF solvents gave good results under HZIF@TCPP-Fe/Fe catalyst (Table 1, Entries 10–13). Thus, HZIF@TCPP-Fe/Fe catalyst was clearly the best catalyst for oxidative dehydrogenation of ethyl 2-phenylhydrazine-1-carboxylate. With the optimal reaction conditions (0.25 mmol 1a, 5 mol % TCPP-Fe/Fe bulk, 4 mL THF under ambient conditions), we evaluated the oxidative dehydrogenation strategy to obtain 2a, the corresponding desired products in good yields (85%) (Table 1, Entry 14). The catalyst performance of HZIF@TCPP-Fe/Fe in various atmosphere was also evaluated (Table 1, Entries 15, 16), compared with air and N₂. HZIF@TCPP-Fe/Fe exhibited the best catalytic effect under O₂ atmosphere. For the above experimental results, we can preliminarily confirm that in the structure of the heterogeneous catalyst, the complex structure of TCPP-Fe/Fe composed with TCPP-Fe and Fe(III) plays the major catalytic role for oxidative dehydrogenation of aromatic hydrazides reaction.

A plausible mechanism for the oxidative dehydrogenation of aromatic hydrazide reaction under HZIF@TCPP-Fe/Fe heterogeneous catalyst is shown in Figure 3a. First, the Fe(III) was reduced to the Fe(II) by the aromatic hydrazides 1(i), and cation radical (ii) was generated. Subsequently, the radical intermediate (iii) was formed by the deprotonation process. Finally, the intermediate (iii) was oxidized by Fe(III) to obtain the product 2 (iv).^[53–55] For effectively improving the catalytic performance, the catalytic active site can be provided in the form of QTD TCPP-Fe/Fe ultra-thin metallized film. As shown in Figure 3b, QTD TCPP-Fe/Fe ultra-thin metallized film formed by deposition of TCPP-Fe chelated with Fe(III) was loaded on the surface of hollow nanocage skeleton. Thus, we have used surface-mounted ultra-thin metallized film grown on suitably functionalized substrates, providing inter digitated bottom contacts. This approach allows the demonstrate of catalytic properties of as-prepared materials in a straightforward fashion. In addition, as shown in Figure 3c, the designed HZIF@TCPP-Fe/Fe catalyst can be easily recovered by centrifugation, the catalyst morphology is generally maintained intact (Figure S13, Supporting Information), and repeatedly used for at least five consecutive reaction cycles with only slight activity loss. To prove that the preparation of QTD TCPP-Fe/Fe film is one of the necessary strategies for preparing the catalyst, Ni(II), Mn(II), Co(II), and Ce(III) were chosen as the coordination metal to prepare other four different catalysts: HZIF@TCPP-Fe/Ni, HZIF@TCPP-Fe/Mn, HZIF@TCPP-Fe/Co, and HZIF@TCPP-Fe/Ce (Figure S14, Supporting Information). The SEM images, EDS mappings and XRD measurements of them are shown in Figures S15 and S16, Supporting Information. From the catalytic results, the introduction of other four transition metals did not achieve the desired catalytic effect in 4 h (Figure S17, Supporting Information). Hence, the development of heterogeneous catalyst with QTD TCPP-Fe/Fe ultra-thin metallized film by cross-linked surface engineering for the oxidative dehydrogenation of aromatic hydrazide is indispensable,

Table 1. Optimization of the reaction conditions.



Entry ^{a)}	Cat.	Solvent	Atmosphere	Time [h]	Yield [%]
1	–	THF	O ₂	24	<1
2	ZIF-8	THF	O ₂	24	<1
3	HZIF	THF	O ₂	24	<1
4	HZIF/NH ₂	THF	O ₂	24	<1
5 ^{b)}	HZIF@Fe(II)	THF	O ₂	24	25
6 ^{c)}	HZIF@Fe(III)	THF	O ₂	24	27
7 ^{d)}	FeCl ₂ ·4H ₂ O	THF	O ₂	24	10
8 ^{e)}	FeCl ₃ ·6H ₂ O	THF	O ₂	24	14
9 ^{f)}	HZIF@TCPP-Fe	THF	O ₂	24	72
10 ^{g)}	HZIF@TCPP-Fe/Fe	THF	O ₂	4	92
11 ^{g)}	HZIF@TCPP-Fe/Fe	CH ₂ Cl ₂	O ₂	4	90
12 ^{g)}	HZIF@TCPP-Fe/Fe	Toluene	O ₂	4	52
13 ^{g)}	HZIF@TCPP-Fe/Fe	Ethyl acetate	O ₂	4	60
14 ^{h)}	TCPP-Fe/Fe bulk	THF	O ₂	4	85
15 ^{g)}	HZIF@TCPP-Fe/Fe	THF	N ₂	4	<1
16 ^{g)}	HZIF@TCPP-Fe/Fe	THF	Air	4	54

^{a)}Reaction conditions: 1 (0.25 mmol), catalysts (5 mol %), solvent (4 mL) at room temperature; ^{b)}5 mol % of HZIF@Fe(II) catalyst; ^{c)}5 mol % of HZIF@Fe(III) catalyst; ^{d)}5 mol % of FeCl₂·4H₂O catalyst; ^{e)}5 mol % of FeCl₃·6H₂O catalyst; ^{f)}5 mol % of HZIF@TCPP-Fe catalyst; ^{g)}5 mol % of HZIF@TCPP-Fe/Fe catalyst; ^{h)}5 mol % of TCPP-Fe/Fe bulk catalyst.

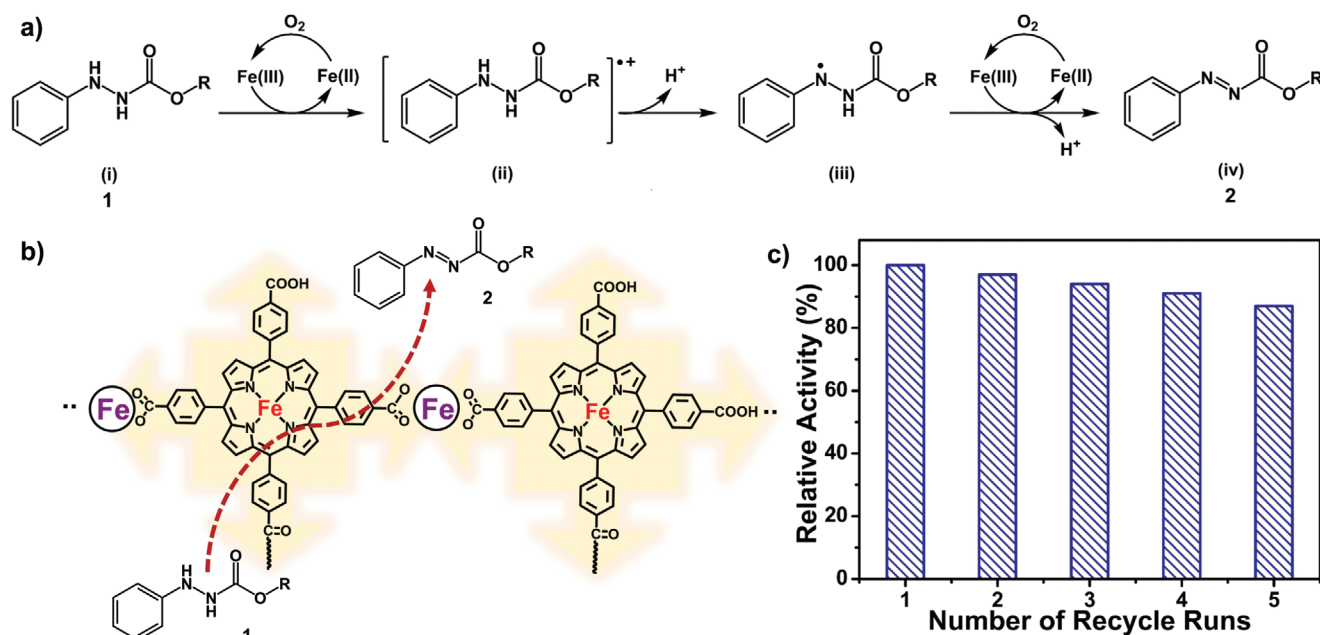


Figure 3. a) Plausible mechanism. b) Scheme of the TCPP-Fe/Fe ultra-thin metallized film catalyzed oxidative dehydrogenation of aromatic hydrazides reactions. c) Catalytic efficiency in the reaction over the five cycles.

because 1) the QTD TCPP-Fe/Fe ultra-thin metallized film constructed by cross-linked surface engineering has abundant unsaturated Fe active sites with excellent accessibility for reaction substrate; 2) the carboxyl group electron-withdrawing substituent electrically shifts $Fe(III)/Fe(II)$ potential to more positive values, increases the rate of reaction with oxygen-active species; 3) the in-situ deposition of ultra-thin metallized films will produce some irregular defects, such as “holes”, increase the roughness and accessibility of the catalyst surface and the probability of contact with the reaction substrate; 4) the hollow skeleton may be employed as nanoscale containers to load small organic molecules. Inspired by these facts, we have synthesized the HZIF@TCPP-Fe/Fe heterogeneous catalyst, for the catalytic oxidative dehydrogenation of aromatic hydrazide reactions. Combine the structural advantages of the catalyst with the hypothetical mechanisms, the outstanding activity of the halogenated HZIF@TCPP-Fe/Fe can be ascribed to the above factors, for the catalytic oxidative dehydrogenation of aromatic hydrazide reactions. With the established optimal reaction conditions in hand (Table 1, Entry 10), substrate scopes were investigated (Table S3, Supporting Information). The as-prepared HZIF@TCPP-Fe/Fe mainly committed the efficient with QTD TCPP-Fe/Fe catalytically active sites and distinguished oxidative dehydrogenation of aromatic hydrazides obviously discloses a reactivity order of primary > secondary > tertiary carbon.

In summary, we have proposed new strategy to prepare a novel kind of highly efficient, robust, and reusable HZIF@TCPP-Fe/Fe heterogeneous catalyst, for the catalytic oxidative dehydrogenation of aromatic hydrazide reactions. The resulting HZIF@TCPP-Fe/Fe has highly dispersed multiple active sites, controllable morphology and ultra-thin metallized film thickness, which have prominent contribution to improving the catalytic performance of the heterogeneous catalyst. The external cross-linked surface engineering of QTD TCPP-Fe/Fe ultra-thin metallized

film has been widely explored, typically by post-synthetic modification methodologies, to endow multifunctionality into hollow skeleton that cannot be directly introduced by de novo syntheses. Thus, this work demonstrates that HZIF@TCPP-Fe/Fe as heterogeneous catalyst can provide a specific environment to determine the main direction of a chemical reaction.

Supporting Information

Supporting Information is available from the Wiley Online Library or from the author.

Acknowledgements

The authors thank the Natural Science Foundation of China (21575115, 21705117); the Program for Chang Jiang Scholars and Innovative Research Team, Ministry of Education, China (IRT-16R61); and the Program of Gansu Provincial Higher Education Research Project (2017-D-01); the Program of Tianjin Science and Technology Major Project and Engineering (19ZXYSY00090).

Conflict of Interest

The authors declare no conflict of interest.

Keywords

aromatic hydrazides, green chemistry, heterogeneous catalysts, iron porphyrin, quasi-two-dimensional films, ultra-thin metallized films

Received: October 15, 2019

Revised: January 18, 2020

Published online:

- [1] S. Horike, S. Shimomura, S. Kitagawa, *Nat. Chem.* **2009**, *1*, 695.
- [2] Z. Cai, Z. Wang, J. Kim, Y. Yamauchi, *Adv. Mater.* **2019**, *31*, 1804903.
- [3] L. Yu, X. Yu, X. Lou, *Adv. Mater.* **2018**, *30*, 1800939.
- [4] W. Zhao, G. Li, Z. Tang, *Nano Today* **2019**, *27*, 178.
- [5] X. Wang, J. Feng, Y. Bai, Q. Zhang, Y. Yin, *Chem. Rev.* **2016**, *116*, 10983.
- [6] L. Chen, R. Luque, Y. Li, *Chem. Soc. Rev.* **2017**, *46*, 4614.
- [7] H. Zhou, J. R. Long, O. M. Yaghi, *Chem. Rev.* **2012**, *112*, 673.
- [8] H. Furukawa, K. E. Cordova, M. O'Keeffe, O. M. Yaghi, *Science* **2013**, *341*, 1230444.
- [9] H. Wang, P. Rassu, X. Wang, H. Li, X. Wang, X. Wang, X. Feng, A. Yin, P. Li, X. Jin, S. Chen, X. Ma, B. Wang, *Angew. Chem., Int. Ed.* **2018**, *57*, 16416.
- [10] Q. Xia, H. Wang, B. Huang, X. Yuan, J. Zhang, J. Zhang, L. Jiang, T. Xiong, G. Zeng, *Small* **2019**, *15*, 1902459.
- [11] W. Zhu, Z. Chen, Y. Pan, R. Dai, Y. Wu, Z. Zhuang, D. Wang, Q. Peng, C. Chen, Y. Li, *Adv. Mater.* **2019**, *31*, 1800426.
- [12] X. Qiao, B. Su, C. Liu, Q. Song, D. Luo, G. Mo, T. Wang, *Adv. Mater.* **2018**, *30*, 1702275.
- [13] M. G. Marqués, E. Bellido, T. Berthelot, T. S. Yarza, T. Hidalgo, R. S. Vázquez, Á. G. Fernández, J. Avila, M. C. Asensio, R. Gref, P. Couvreur, C. Serre, P. Horcajada, *Small* **2018**, *14*, 1801900.
- [14] M. Pinaut, V. Picholt, H. Khoda, P. Launois, C. Reynaud, M. M. L'Hermite, *Nano Lett.* **2005**, *5*, 2394.
- [15] Z. Xue, P. Wang, A. Peng, T. Wang, *Adv. Mater.* **2019**, *31*, 1801441.
- [16] P. Elumalai, H. Mamlouk, W. Yiming, L. Feng, S. Yuan, H. Zhou, S. T. Madrahimov, *ACS Appl. Mater. Interfaces* **2018**, *10*, 41431.
- [17] S. T. Madrahimov, J. R. Gallagher, G. Zhang, Z. Meinhart, S. J. Garibay, M. Delferro, J. T. Miller, O. K. Farha, J. T. Hupp, S. T. Nguyen, *ACS Catal.* **2015**, *5*, 6713.
- [18] L. Feng, S. Yuan, J. L. Li, K. Y. Wang, G. S. Day, P. Zhang, Y. Wang, H. C. Zhou, *ACS Cent. Sci.* **2018**, *4*, 1719.
- [19] S. Zhang, B. Zhang, H. Liang, Y. Liu, Y. Qiao, Y. Qin, *Angew. Chem., Int. Ed.* **2018**, *57*, 1091.
- [20] M. Hu, S. Zhao, S. Liu, C. Chen, W. Chen, W. Zhu, C. Liang, W. Cheong, Y. Wang, Y. Yu, Q. Peng, K. Zhou, J. Li, Y. Li, *Adv. Mater.* **2018**, *30*, 1801878.
- [21] N. Huang, S. Yuan, H. Drake, X. Yang, J. Pang, J. Qin, J. Li, Y. Zhang, Q. Wang, D. Jiang, H. Zhou, *J. Am. Chem. Soc.* **2017**, *139*, 18590.
- [22] L. Feng, Y. Wang, S. Yuan, K. Wang, J. Li, G. S. Day, D. Qiu, L. Cheng, W. Chen, S. T. Madrahimov, H. Zhou, *ACS Catal.* **2019**, *9*, 5111.
- [23] G. Li, S. Zhao, Y. Zhang, Z. Tang, *Adv. Mater.* **2018**, *30*, 1800702.
- [24] Y. Wang, H. Cui, Z. Wei, H. Wang, L. Zhang, C. Su, *Chem. Sci.* **2017**, *8*, 775.
- [25] R. Yang, R. Li, Y. Cao, Y. Wei, Y. Miao, W. Tan, X. Jiao, H. Chen, L. Zhang, Q. Chen, H. Zhang, W. Zou, Y. Wang, M. Yang, C. Yi, N. Wang, F. Gao, C. R. McNeill, T. Qin, J. Wang, W. Huang, *Adv. Mater.* **2018**, *30*, 1804771.
- [26] S. G. Kwon, G. Krylova, A. Sumer, M. M. Schwartz, E. E. Bunel, C. L. Marshall, S. Chattopadhyay, B. Lee, J. Jellinek, E. V. Shevchenko, *Nano Lett.* **2012**, *12*, 5382.
- [27] Z. Niu, Y. Li, *Chem. Mater.* **2014**, *26*, 72.
- [28] X. Ning, B. Lu, Z. Zhang, P. Du, H. Ren, D. Shan, J. Chen, Y. Gao, X. Lu, *Angew. Chem., Int. Ed.* **2019**, *58*, 16800.
- [29] X. Ning, Y. Wu, X. Ma, Z. Zhang, R. Gao, J. Chen, D. Shan, X. Lu, *Adv. Funct. Mater.* **2019**, *29*, 1902992.
- [30] X. Ning, W. Li, Y. Meng, D. Qin, J. Chen, X. Mao, Z. Xue, D. Shan, S. Devaramani, X. Lu, *Small* **2018**, *14*, 1703989.
- [31] Y. Li, Z. Gao, F. Chen, C. You, H. Wu, K. Sun, P. An, K. Cheng, C. Sun, X. Zhu, B. Sun, *ACS Appl. Mater. Interfaces* **2018**, *10*, 30930.
- [32] L. Feng, S. Yuan, L. Zhang, K. Tan, J. Li, A. Kirchon, L. Liu, P. Zhang, Y. Han, Y. J. Chabal, H. Zhou, *J. Am. Chem. Soc.* **2018**, *140*, 2363.
- [33] L. Liu, Z. Chen, J. Wang, D. Zhang, Y. Zhu, S. Ling, K. Huang, Y. Belmabkhout, K. Adil, Y. Zhang, B. Slater, M. Eddaoudi, Y. Han, *Nat. Chem.* **2019**, *11*, 622.
- [34] M. Guo, J. Balamurugan, X. Li, N. H. Kim, J. H. Lee, *Small* **2017**, *13*, 1701275.
- [35] L. Tang, S. Zhang, Q. Wu, X. Wang, H. Wu, Z. Jiang, *J. Mater. Chem. A* **2018**, *6*, 2964.
- [36] F. Zhang, Y. Wei, X. Wu, H. Jiang, W. Wang, H. Li, *J. Am. Chem. Soc.* **2014**, *136*, 13963.
- [37] L. An, J. Feng, Y. Zhang, Y. Zhao, R. Si, G. Wang, F. Cheng, P. Xi, S. Sun, *Nano Energy* **2019**, *57*, 644.
- [38] Y. Wang, M. Zhao, J. Ping, B. Chen, X. Cao, Y. Huang, C. Tan, Q. Ma, S. Wu, Y. Yu, Q. Lu, J. Chen, W. Zhao, Y. Ying, H. Zhang, *Adv. Mater.* **2016**, *28*, 4149.
- [39] Z. Wang, H. Jin, T. Meng, K. Liao, W. Meng, J. Yang, D. He, Y. Xiong, S. Mu, *Adv. Funct. Mater.* **2018**, *28*, 1802596.
- [40] Y. Wang, D. Adekoya, J. Sun, T. Tang, H. Qiu, L. Xu, S. Zhang, Y. Hou, *Adv. Funct. Mater.* **2019**, *29*, 1807485.
- [41] L. Jiao, G. Wan, R. Zhang, H. Zhou, S. Yu, H. Jiang, *Angew. Chem., Int. Ed.* **2018**, *57*, 8525.
- [42] Y. Huang, M. Zhao, S. Han, Z. Lai, J. Yang, C. Tan, Q. Ma, Q. Lu, J. Chen, X. Zhang, Z. Zhang, B. Li, B. Chen, Y. Zong, H. Zhang, *Adv. Mater.* **2017**, *29*, 1700102.
- [43] M. Zhang, Q. Shang, Y. Wan, Q. Cheng, G. Liao, Z. Pan, *Appl. Catal., B* **2019**, *241*, 149.
- [44] P. T. Wong, S. K. Choi, *Chem. Rev.* **2015**, *115*, 3388.
- [45] D. Hirose, T. Taniguchi, H. Ishibashi, *Angew. Chem., Int. Ed.* **2013**, *52*, 4613.
- [46] A. B. Sorokin, *Chem. Rev.* **2013**, *113*, 8152.
- [47] E. Wang, Y. Ping, Z. Li, H. Qin, Z. Xu, C. Che, *Org. Lett.* **2018**, *20*, 4641.
- [48] D. Hirose, M. Gazvoda, J. Košmrlj, T. Taniguchi, *Org. Lett.* **2016**, *18*, 4036.
- [49] D. Hirose, M. Gazvoda, J. K. Smrlj, T. Taniguchi, *Chem. Sci.* **2016**, *7*, 5148.
- [50] R. Jiang, L. Li, T. Sheng, G. Hu, Y. Chen, L. Wang, *J. Am. Chem. Soc.* **2018**, *140*, 11594.
- [51] J. Yi, R. Xu, Q. Wu, T. Zhang, K. Zang, J. Luo, Y. Liang, Y. Huang, R. Cao, *ACS Energy Lett.* **2018**, *3*, 883.
- [52] T. Hashimoto, D. Hirose, T. Taniguchi, *Adv. Synth. Catal.* **2015**, *357*, 3346.
- [53] T. Taniguchi, D. Hirose, H. Ishibashi, *ACS Catal.* **2011**, *1*, 1469.
- [54] X. Wang, X. Wang, C. Xia, L. Wu, *Green Chem.* **2019**, *21*, 4189.
- [55] T. Taniguchi, Y. Sugiura, H. Zaimoku, H. Ishibashi, *Angew. Chem., Int. Ed.* **2010**, *49*, 10154.